Balance Control With Relative Angular Momentum/Velocity

○ Yoshikazu Kanamiya

1. Introduction

The concept and realization of a balance controller based on the spatial momentum of a humanoid robot was introduced by Kajita et al. [1]. The *resolved momentum* framework was the result of a pioneering effort toward a velocity-based *whole-body* balance control. The control law formulation was flawed, however, since the reference base-link twist was constrained by the null space of the main subtask. This led to an undesirable upper-body rotation. In addition, task conflicts occurred that led to instabilities. The important role of *centroidal angular momentum* and its rate of change in balance control of humanoid robots was discussed in [2]. It was shown that the presence of centroidal angular momentum is equivalent to shifting the application point of the ground reaction force (GRF) to a special point called the *centroidal moment pivot* (CMP) [3]. Further insight into the role of the angular momentum component and its relation to the widely used inverted pendulum models was provided in [4,5] with a simple inverted pendulum plus a *reaction wheel* model. Since then, a number of researchers began to develop balance controllers with angular momentum control components. The most recent results in balance control [6–8] have confirmed the importance of the centroidal angular momentum, not only for walking on a flat ground, but also while stepping on a highly irregular terrain. From this brief overview it can be concluded that the centroidal angular momentum control is an indispensable component in the whole-body balance control of a humanoid robot.

In this work it is argued that although necessary, the centroidal angular momentum balance control approach is not sufficient. This hypothesis is based on the fact that the centroidal angular momentum can be expressed as the sum of two components: a composite rigid body (CRB) component that is determined by a system state with locked joints, and the *coupling angular momentum* (CAM) component that depends on the joint rates. The joint rates are mapped via the coupling inertia matrix. The role of the CAM component in the design of controllers for various underactuated robots on a floating-base, e.g. free-floating space robots, manipulators mounted on a flexible base and macro-mini manipulators (i.e. a small-size manipulator mounted at the tip of a large-size one) is discussed in [9].

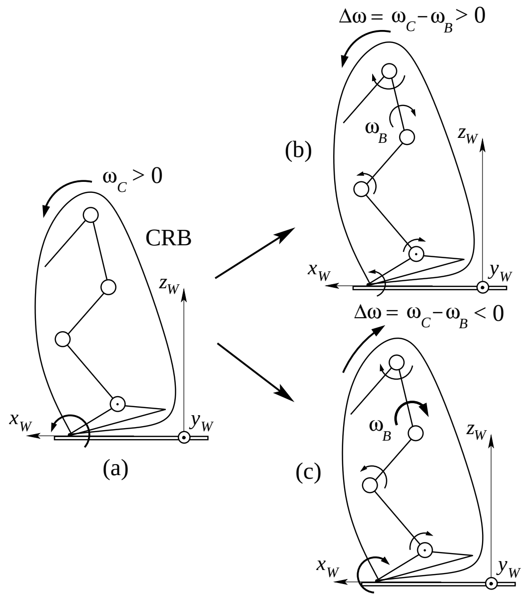

Fig. 1 Stabilization with the relative angular velocity.

The reason why so far little attention has been paid to the CAM in the field of humanoid robotics is that most formulations have been based on the theoretical analysis with the *centroidal momentum matrix* [10, 11]. The analysis does not account for the existence of the CAM component.

The aim of this work is twofold. First, it will be shown that based on the CAM, a whole-body balance controller can be designed that is capable of tracking the reference CRB trajectories with asymptotic stability, as long as the contacts are maintained. The reference CRB trajectories comprise two components; one for the reference center-of-mass (CoM) translational motion and another one for the reference rotation of the base link. The two components can be designed *independently*. Second, it will be shown that with an additional reference input, the motion of the arms can be controlled in a way to ensure such objectives as centroidal or coupling angular momentum conservation. The latter is derived from the *reaction null space* (RNS) [9]. It will also be shown that in this case, the controller is endowed with a *self-stabilization* property, allowing the robot to handle unstable states (e.g. foot roll) without any additional provisions.

2. Background and notation

The generalized coordinate vector of a floating-base robot is denoted by $\boldsymbol{q} = (\mathcal{X}_M, \boldsymbol{\theta})$. $\boldsymbol{\theta} \in \Re^n$ stands for the joint variable vector, $\mathcal{X}_M \in SE(3)$ is the position of the CoM and the orientation of the (non-actuated) base link. The generalized velocity of the robot is defined as a *quasi-velocity*: $\dot{\boldsymbol{q}}_M = \begin{bmatrix}\mathcal{V}_M^T & \dot{\boldsymbol{\theta}}^T\end{bmatrix}^T$, where $\mathcal{V}_M = \begin{bmatrix}\boldsymbol{v}_C^T & \boldsymbol{\omega}_B^T\end{bmatrix}^T$, $\boldsymbol{v}_C, \boldsymbol{\omega}_B \in \Re^3$ standing for the velocity of the CoM and and the angular velocity of the base link. Note that there is some abuse in the notation: the over-dot in $\dot{\boldsymbol{q}}_M$ does not necessarily imply the integrability of this quantity.

Further on, note that the centroidal spatial momentum of the robot can be expressed in different ways. First, consider the joints-locked case. The centroidal spatial momentum of the CRB is defined as $\mathcal{L}_C = \begin{bmatrix}\boldsymbol{p}^T & \boldsymbol{l}_C^T\end{bmatrix}^T$ where $\boldsymbol{p} = M\boldsymbol{v}_C$ and $\boldsymbol{l}_C = \boldsymbol{I}_C(\boldsymbol{q})\boldsymbol{\omega}_C$ denote the linear and the centroidal angular momentum components, respectively. M is the total mass, $\boldsymbol{I}_C(\boldsymbol{q}) \in \in \Re^{3\times 3}$ stands for the centroidal inertia tensor. Thus,

$$\mathcal{L}_C = \mathbb{M}_C(\boldsymbol{q})\mathcal{V}_C \tag{1}$$

where $\mathcal{V}_C = \begin{bmatrix}\boldsymbol{v}_C^T & \boldsymbol{\omega}_C^T\end{bmatrix}^T$ and

$$\mathbb{M}_C(\boldsymbol{q}) \equiv \begin{bmatrix} M\boldsymbol{E} & \boldsymbol{0} \\ \boldsymbol{0} & \boldsymbol{I}_C(\boldsymbol{q}) \end{bmatrix} \in \Re^{6\times 6}$$

is the spatial inertia tensor of the CRB. $\boldsymbol{E}$ denotes the identity matrix. The expression of the centroidal spatial momentum in terms of the $\dot{\boldsymbol{q}}_M$ defined above is:

$$\begin{aligned}\mathcal{L}_C(\boldsymbol{q}, \dot{\boldsymbol{q}}_M) &= \mathcal{L}_{CM}(\boldsymbol{q}, \mathcal{V}_M) + \mathcal{L}_{C\theta}(\boldsymbol{q}, \dot{\boldsymbol{\theta}}) \\ &= \mathbb{M}_C\mathcal{V}_M + \boldsymbol{H}_{CM}\dot{\boldsymbol{\theta}} \qquad (2) \\ &= \begin{bmatrix} M\boldsymbol{E} & \boldsymbol{0} \\ \boldsymbol{0} & \boldsymbol{I}_C \end{bmatrix}\begin{bmatrix}\boldsymbol{v}_C \\ \boldsymbol{\omega}_B\end{bmatrix} + \begin{bmatrix}\boldsymbol{0} \\ \boldsymbol{H}_C\end{bmatrix}\dot{\boldsymbol{\theta}}. \qquad (3)\end{aligned}$$

Matrix $\boldsymbol{H}_C(\boldsymbol{q}) \in \Re^{3\times n}$, appearing in the *coupling spatial momentum* component $\mathcal{L}_{CM}(\boldsymbol{q}, \dot{\boldsymbol{\theta}})$, is a joint velocity to angular momentum map. It is important to distinguish between the *system spatial momentum* $\mathcal{L}_C$ and the *CRB spatial momentum* $\mathcal{L}_{CM}(\boldsymbol{q}, \mathcal{V}_M)$; they are not equal, unless the joints are locked.

From (3) it is apparent that the linear momentum is completely decoupled from the joint velocity. This property yields an advantage in balance controller design, as already clarified in [12], and also in [13].

2.1 Instantaneous motion constraints

The instantaneous motion of the robot is constrained by c constraints at the contact joints, such that

$$\mathbb{C}_c^T(\boldsymbol{q})\mathcal{V}_M + \mathcal{J}_c(\boldsymbol{q})\dot{\boldsymbol{\theta}} = \boldsymbol{0}. \tag{4}$$

$\mathbb{C}_c(\boldsymbol{q}) \in \Re^{6\times c}$ and $\mathcal{J}_c(\boldsymbol{q}) \in \Re^{c\times n}$ denote the contact map and the Jacobian in the constrained-motion directions, respectively. Furthermore, there are η unconstrained-motion directions. The respective instantaneous motion is determined by:

$$\mathbb{C}_m^T(\boldsymbol{q})\mathcal{V}_M + \mathcal{J}_m(\boldsymbol{q})\dot{\boldsymbol{\theta}} = \bar{\mathcal{V}}^m. \tag{5}$$

$\mathbb{C}_m(\boldsymbol{q}) \in \Re^{6\times \eta}$ and $\mathcal{J}_m(\boldsymbol{q}) \in \Re^{\eta\times n}$ denote the contact map and the Jacobian in the mobility (unconstrained-motion) directions, respectively. $\bar{\mathcal{V}}^m \in \Re^\eta$ are the twist components for the instantaneous end-link motion along the unconstrained motion directions [14].

3. The momentum equilibrium principle in balance control

With the help of (1), relation (2) becomes:

$$\boldsymbol{H}_{CM}\dot{\boldsymbol{\theta}} = \mathbb{M}_C\mathcal{V}_C - \mathbb{M}_C\mathcal{V}_M. \tag{6}$$

This relation clearly shows that the quantity that can be controlled via the joint velocity, is of relative character. This quantity will be referred to as the *relative spatial momentum* of the system.

The above equation represents the momentum equilibrium principle in balance control: *the coupling momentum is always in a dynamic equilibrium with the relative momentum.* The principle is quite helpful in balance controller design. In fact, it has been exploited throughout the years, but only with regard to the linear momentum component.

Noting that $\mathbb{M}_C$ is positive definite, the momentum equilibrium principle (6) can be rewritten in terms of spatial velocity:

$$\mathbb{M}_C^{-1}\boldsymbol{H}_{CM}\dot{\boldsymbol{\theta}} = \mathcal{V}_C - \mathcal{V}_M \equiv \Delta\mathcal{V}. \tag{7}$$

The term on the left hand-side, referred to as the *coupling spatial velocity*, is in balance with the *relative spatial velocity* $\Delta\mathcal{V}$ on the right hand-side.

The above relation is represented componentwise as:

$$\boldsymbol{0} = \boldsymbol{v}_{C_R} - \boldsymbol{v}_{C_I}, \tag{8}$$

$$\boldsymbol{J}_\omega\dot{\boldsymbol{\theta}} = \boldsymbol{\omega}_C - \boldsymbol{\omega}_B \equiv \Delta\boldsymbol{\omega} \tag{9}$$

where $\boldsymbol{J}_\omega(\boldsymbol{\theta}) = \boldsymbol{I}_C^{-1}(\boldsymbol{q})\boldsymbol{H}_C(\boldsymbol{q})$ and $\boldsymbol{\omega}_C = \boldsymbol{I}_C^{-1}\boldsymbol{l}_C$. The notation in the upper equation clarifies that the coupling CoM velocity is zero. It also clarifies that the CoM velocity can be interpreted in two ways: $\boldsymbol{v}_{C_I}$ is of *inertial* origin, while $\boldsymbol{v}_{C_R}$ stems from the *net* system twist that is of *reactive* origin. Next, note that the lower equation expresses a dynamic equilibrium in the angular velocities: the *coupling angular velocity* $\boldsymbol{J}_\omega\dot{\boldsymbol{\theta}}$ is in balance with the *relative angular velocity* (RAV) $\Delta\boldsymbol{\omega} \neq \boldsymbol{0}$. One arrives then at the important conclusion that *the angular velocity of the system and that of the base link can be assigned in an independent way.* The RAV plays an important role in the stabilization of unstable states. The concept is outlined in Fig. 1, the details will be given below.

4. CRB motion trajectory tracking with asymptotic stability

It is assumed that the reference values for the CoM velocity and the two angular velocities $\boldsymbol{\omega}_C$ and $\boldsymbol{\omega}_B$ are known from the task assignment. The joint rates can then be determined from the coupling angular velocity in (9), by solving a least-squares optimization task. The desired trajectories of the CRB twist, $\mathcal{V}_M^{des} = \begin{bmatrix}(\boldsymbol{v}_C^{des})^T & (\boldsymbol{\omega}_B^{des})^T\end{bmatrix}^T$, can be tracked with a conventional velocity tracking controller. The constraint-consistent joint velocity solution is obtained from (4) as:

$$\dot{\boldsymbol{\theta}}_1 = -\boldsymbol{\mathcal{J}}_c^{+}\mathbb{C}_c^{T}\mathcal{V}_M^{ref} + \boldsymbol{N}(\boldsymbol{\mathcal{J}}_c)\,\dot{\boldsymbol{\theta}}_u. \tag{10}$$

$(\circ)^+$ denotes the pseudoinverse. The second term on the right-hand side is a null-space term: $\boldsymbol{N}(\circ)$ denotes a projector onto the null space, in this case of the contact Jacobian. $\dot{\boldsymbol{\theta}}_u$ is an arbitrary joint velocity that parameterizes the null space. $\mathcal{V}_M^{ref}$ comprises *independent* feedforward/feedback control components

$$\boldsymbol{v}_C^{ref} = \boldsymbol{v}_C^{des} + K_{pC}\boldsymbol{e}_{pC} \tag{11}$$

$$\boldsymbol{\omega}_B^{ref} = \boldsymbol{\omega}_B^{des} + K_{oB}\boldsymbol{e}_{oB}, \tag{12}$$

$\boldsymbol{e}_{pC} = \boldsymbol{r}_C^{des} - \boldsymbol{r}_C$ and $\boldsymbol{e}_{oB}$ denoting the CoM position error and the orientation error of the base link, respectively. The control law (10) guarantees that $\mathcal{V}_M(t) = \mathcal{V}_M^{ref}(t)$ asymptotically, provided the contact states are maintained and the joint-space constraint Jacobian $\boldsymbol{\mathcal{J}}_c$ is full (row) rank.

The control input $\dot{\boldsymbol{\theta}}_1$ is useful in case of a double stance. In a single stance, the swing-foot motion control task could be embedded as a lower-priority task. To this end, determine the arbitrary joint velocity vector $\dot{\boldsymbol{\theta}}_u$ in (10) using the instantaneous-motion equation (5). The control joint velocity assumes then the form:

$$\dot{\boldsymbol{\theta}}_2 = -\boldsymbol{\mathcal{J}}_c^{+}\mathbb{C}_c^{T}\mathcal{V}_M^{ref} + \overline{\boldsymbol{\mathcal{J}}}_m^{+}(\widetilde{\mathcal{V}}^{m})^{ref} + \boldsymbol{N}(\boldsymbol{\mathcal{J}}_c)\boldsymbol{N}(\overline{\boldsymbol{\mathcal{J}}}_m)\dot{\boldsymbol{\theta}}_u \tag{13}$$

where $\overline{\boldsymbol{\mathcal{J}}}_m = \boldsymbol{\mathcal{J}}_m\boldsymbol{N}(\boldsymbol{\mathcal{J}}_c)$ is the restricted end-link mobility Jacobian and

$$(\widetilde{\mathcal{V}}^{m})^{ref} = (\overline{\mathcal{V}}^{m})^{ref} + \left(\boldsymbol{\mathcal{J}}_m\boldsymbol{\mathcal{J}}_c^{+}\mathbb{C}_c^{T} - \mathbb{C}_m^{T}\right)\mathcal{V}_M^{ref}.$$

$(\overline{\mathcal{V}}^{m})^{ref}$ comprises a nonzero component for the swing leg:

$$\mathcal{V}_{SW}^{ref} = \mathcal{V}_{SW}^{des} + \boldsymbol{K}_{SW}\mathcal{E}_{SW}, \tag{14}$$

the rest of the components of $(\overline{\mathcal{V}}^{m})^{ref}$ are zeros. Subscript SW stands for the swing leg, $\mathcal{E}_{SW}$ is the error twist, $\boldsymbol{K}_{SW}$ is a p.d. feedback gain. Note that control input $\dot{\boldsymbol{\theta}}_2$ can also be used in the case of a double stance, by adjusting the constraint conditions appropriately.

5. Balance control

To obtain a controller with an enhanced balance control capability, add a term for controlling the centroidal angular momentum, via the system (centroidal) angular velocity $\boldsymbol{\omega}_C$. Insert (13) into (9) and solve for the arbitrary $\dot{\boldsymbol{\theta}}_u$. Then, insert back into (10) to finally obtain the enhanced control law as:

$$\begin{aligned}\dot{\boldsymbol{\theta}} &= -\boldsymbol{\mathcal{J}}_c^{+}\mathbb{C}_c^{T}\mathcal{V}_M^{ref} + \overline{\boldsymbol{\mathcal{J}}}_m^{+}(\widetilde{\mathcal{V}}^{m})^{ref} + \overline{\boldsymbol{J}}_\omega^{+}\left(\Delta\boldsymbol{\omega}^{ref} - \tilde{\boldsymbol{\omega}}\right)\\ &\quad + \boldsymbol{N}(\boldsymbol{\mathcal{J}}_c)\boldsymbol{N}(\overline{\boldsymbol{\mathcal{J}}}_m)\boldsymbol{N}(\overline{\boldsymbol{J}}_\omega)\,\dot{\boldsymbol{\theta}}_u^{ref} \qquad (15)\\ &= \dot{\boldsymbol{\theta}}^{c} + \dot{\boldsymbol{\theta}}^{m} + \dot{\boldsymbol{\theta}}^{am} + \dot{\boldsymbol{\theta}}^{n}\end{aligned}$$

where $\Delta\boldsymbol{\omega}^{ref} = \boldsymbol{\omega}_C^{ref} - \boldsymbol{\omega}_B^{ref}$ and

$$\begin{aligned}\overline{\boldsymbol{J}}_\omega &= \boldsymbol{J}_\omega\boldsymbol{N}(\boldsymbol{\mathcal{J}}_c)\boldsymbol{N}(\overline{\boldsymbol{\mathcal{J}}}_m),\\ \tilde{\boldsymbol{\omega}} &= \boldsymbol{J}_\omega\left(-\boldsymbol{\mathcal{J}}_c^{+}\mathbb{C}_c^{T}\mathcal{V}_M^{ref} + \overline{\boldsymbol{\mathcal{J}}}_m^{+}(\widetilde{\mathcal{V}}^{m})^{ref}\right).\end{aligned}$$

The control input $\dot{\boldsymbol{\theta}}$ in the last equation is composed of four components arranged in hierarchical order. The highest-priority component, $\dot{\boldsymbol{\theta}}^{c}$, is used to control the instantaneous motion of the CRB, via the contact constraints. The desired CRB translational (i.e. of the CoM) and rotational (of the base link) motion is achieved via the movements in the leg(s). The rest of the control components are derived from within the null space $\mathcal{N}(\boldsymbol{\mathcal{J}}_c)$. These components will not disturb the main (the CRB) control task. The role of the second term, $\dot{\boldsymbol{\theta}}^{m}$, is to control the desired motion of the swing-leg, when the robot is in a single stance. The role of the third term, $\dot{\boldsymbol{\theta}}^{am}$, is to control the system (centroidal) angular velocity in a way to ensure an appropriate inertial coupling w.r.t. the desired CRB rotational motion. Such coupling can only be achieved via motion in the arms since the legs and the upper body are controlled by the first two components. The last, fourth component, $\dot{\boldsymbol{\theta}}^{n}$, is used to enforce the joint velocity/angular constraints. To this end, the additional control input $\dot{\boldsymbol{\theta}}_u^{ref}$ can be determined via the gradient projection approach with the joint-limit avoidance potential function introduced e.g. in [15].

Note that when the robot is in a single stance and there is no desired motion task for the swing leg, the second component, $\dot{\boldsymbol{\theta}}^{m}$, becomes irrelevant. The motion of the swing leg will then be determined by the angular momentum component $\dot{\boldsymbol{\theta}}^{am}$. This means that the motion of the swing leg will contribute to postural stabilization, as does the motion in the arms. This contribution plays an important role when a large external disturbance is applied to the robot, as will be shown in the companion paper [16].

The above controller will be referred to as the *relative angular momentum/velocity (RAM/V) controller*. The block diagram of the controller is shown in Fig. 2. The desired values for the CoM motion, the base-link rotation, the swing-leg motion and the centroidal angular momentum can be specified in an *independent* way. The controller does not account for other important constraints, such as keeping the ZMP within the support polygon or the friction cone constraints. But it provides means to avoid destabilization, via an appropriate arm (and possibly swing leg) motion generated by the RAV control input $\Delta\boldsymbol{\omega}^{ref}$. With an appropriate RAV control input, to be determined below, the controller will be endowed with a *self-stabilization* property such that the stability can be recovered even when the state is destabilized by an infeasible CRB motion input or by an external disturbance of large magnitude.

6. RAV control input

A straightforward (but conservative) approach to deal with the coupling problem in balance control is to constrain the motion of the robot within the system angular momentum conserving (at zero) subset of motion. From (9):

$$\boldsymbol{\omega}_C = \boldsymbol{\omega}_B + \boldsymbol{J}_\omega(\boldsymbol{\theta})\dot{\boldsymbol{\theta}} \tag{16}$$

$$= \hat{\boldsymbol{J}}_\omega(\boldsymbol{\theta})\dot{\boldsymbol{q}}_\omega \tag{17}$$

where $\hat{\boldsymbol{J}}_\omega = \begin{bmatrix}\boldsymbol{E} & \boldsymbol{J}_\omega\end{bmatrix}$, $\dot{\boldsymbol{q}}_\omega = (\boldsymbol{\omega}_B, \dot{\boldsymbol{\theta}})$. The system angular momentum is conserved within the set:

$$\{\dot{\boldsymbol{q}}_{\overline{\omega}} \in \mathcal{N}(\hat{\boldsymbol{J}}_\omega) : \dot{\boldsymbol{q}}_\omega = \boldsymbol{N}(\hat{\boldsymbol{J}}_\omega(\boldsymbol{\theta}))\dot{\boldsymbol{q}}_{\omega a},\ \forall \dot{\boldsymbol{q}}_{\omega a}\}. \tag{18}$$

To achieve this, in the RAM/V controller (15) simply set the reference system angular velocity at zero throughout the motion:

$$\boldsymbol{\omega}_C^{ref}(t) = \boldsymbol{0} \ \Rightarrow \Delta\boldsymbol{\omega}^{ref} = \boldsymbol{\omega}_B^{ref} = \boldsymbol{\omega}_B^{des} + K_{o_B}\boldsymbol{e}_{o_B}. \tag{19}$$

This means that the ZMP will depend only on the CoM stabilization task; the ZMP will not be disturbed by the angular momentum task (i.e. the desired base-link rotation).

Another possible approach is to conserve the CAM at zero. This is done within the following joint velocity subset:

$$\{\dot{\boldsymbol{\theta}}_{cam} \in \mathcal{N}(\boldsymbol{J}_\omega) : \dot{\boldsymbol{\theta}} = \boldsymbol{N}(\boldsymbol{J}_\omega(\boldsymbol{\theta}))\dot{\boldsymbol{\theta}}_a,\ \forall \dot{\boldsymbol{\theta}}_a\}.$$

The null-space $\mathcal{N}(\boldsymbol{J}_\omega(\boldsymbol{\theta}))$ is referred to as the (angular momentum) Reaction Null-Space (RNS) [9].

To conserve the coupling angular momentum, in the RAM/V controller (15) simply set the reference system angular velocity to be equal to the base angular velocity throughout the motion:

$$\boldsymbol{\omega}_C^{ref} = \boldsymbol{\omega}_B^{ref} \ \Rightarrow \Delta\boldsymbol{\omega}^{ref} = \boldsymbol{0}. \tag{20}$$

The resulting motion endows the RAM/V controller with the important property of *self-stabilization through angular momentum damping*. This property becomes apparent when the RAM/V controller is rewritten in terms of acceleration under the consideration of integrability [16].

7. RNS-based stabilization of unstable postures

Assume the robot has been destabilized, either proactively or by an external force. This means that the foot (when in a single stance) or the feet (when in a double stance) have begun to roll. A swift action is required for contact stabilization. Such action can be generated in a straightforward way with the RAM/V controller introduced in the previous subsection. This will be explained with the help of the simple sagittal-plane model shown in Fig. 1. Assume the foot rolls around the toe tip counterclockwise, s.t. the system angular speed $\omega_C > 0$, in the chosen coordinate frame. When the joints are locked, $\omega_C = \omega_B$ is the angular speed of the CRB. Also, the relative angular speed is zero: $\Delta\omega = \omega_C - \omega_B = 0$. When the robot links are allowed to rotate, in general the system angular speed will be different from that of the base link, and thus, the relative angular speed will be nonzero. For this particular example, when $\Delta\omega > 0$, the foot roll will persist and result in a fall. On the other hand, when $\Delta\omega < 0$, the foot will start rotating in the opposite (clockwise) direction resulting in the recovery of the line contact, and eventually, of a stable posture.

7.1 Stabilization of postures with rolling feet

The above strategy for contact stabilization of a rolling foot can be realized by making use of the error term in the control law for base-link rotation (12), $K_{o_B}\boldsymbol{e}_{o_B}$[1]. To this end, set

$$\boldsymbol{\omega}_C^{ref} = \boldsymbol{\omega}_B^{des} \ \Rightarrow \Delta\boldsymbol{\omega}^{ref} = -K_{o_B}\boldsymbol{e}_{o_B}. \tag{21}$$

With the above setting, the arm rotation generated via the RAV $\Delta\boldsymbol{\omega}^{ref}$ will be always opposite to that of the foot/CRB roll. At some point in time the foot contact condition will be recovered. Then, the contact constraints will enforce the base-link rotation in accordance with control law (12). Note that the recovery of the contact condition happens only instantaneously since there is no damping. As a consequence, the above stabilization control will yield a rocking-feet motion that does not converge to a stable posture, though. The reason is that the above $\boldsymbol{\omega}_C^{ref}$ represents a *non-collocated* control input [17] to the controller. In this example, the problem can be alleviated in a straightforward way by designing the control input as collocated. This is done by simply reformulating the error term w.r.t. the foot orientation instead to that of the base-link:

$$\Delta\boldsymbol{\omega}^{ref} = -K_{o_F}\boldsymbol{e}_{o_F} \tag{22}$$

where $\boldsymbol{e}_{o_F}$ is the foot orientation error and K_{o_F} is a p.d. feedback gain. Note that the foot rotation angle

[1]Note that to obtain the current base-link orientation, an IMU sensor attached to the base link has to be used.

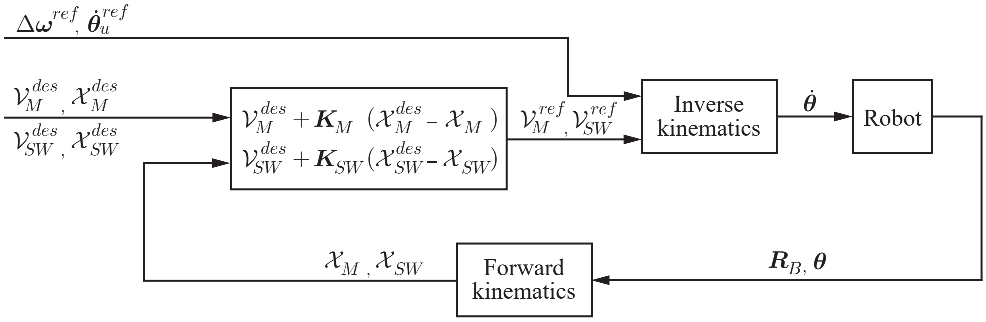

Fig. 2 Block diagram of the RAM/V controller. The Inverse kinematics block calculates the control joint velocity in accordance with (15). The $(\circ)_{SW}$ components are used only when in a single stance. $\boldsymbol{R}_B$ denotes the orientation of the base link.

should be measured directly, e.g. by an IMU sensor placed on the foot.

Control switching and an IMU attached to the foot is somewhat inconvenient. These problems can be avoided when there is damping in the system, as shown in [18]. Damping can also be injected via the control, when the controller is rewritten in terms of acceleration [16].

References

[1] S. Kajita, F. Kanehiro, K. Kaneko, K. Fujiwara, K. Harada, K. Yokoi, and H. Hirukawa. Resolved momentum control: humanoid motion planning based on the linear and angular momentum. In *IEEE/RSJ International Conference on Intelligent Robots and Systems*, pages 1644–1650, Las, Vegas, Nevada, 2003.

[2] A. Goswami and V. Kallem. Rate of change of angular momentum and balance maintenance of biped robots. In *IEEE International Conference on Robotics and Automation*, pages 3785–3790, New Orleans, LA, USA, 2004.

[3] M. B. Popovic, A. Goswami, and H. Herr. Ground reference points in legged locomotion: Definitions, biological trajectories and control implications. *The International Journal of Robotics Research*, 24(12):1013–1032, dec 2005.

[4] J. E. Pratt. *Exploiting inherent robustness and natural dynamics in the control of bipedal walking robots*. PhD thesis, MIT, 2000.

[5] J. Pratt, J. Carff, S. Drakunov, and A. Goswami. Capture point: A step toward humanoid push recovery. In *IEEE-RAS International Conference on Humanoid Robots*, pages 200–207, Genoa, Italy, dec 2006.

[6] J. Englsberger, C. Ott, and A. Albu-Schaffer. Three-dimensional bipedal walking control using Divergent Component of Motion. In *IEEE/RSJ International Conference on Intelligent Robots and Systems*, pages 2600–2607, nov 2013.

[7] J. Englsberger, C. Ott, and A. Albu-Schaffer. Three-dimensional bipedal walking control based on divergent component of motion. *IEEE Transactions on Robotics*, 31(2):355–368, apr 2015.

[8] G. Wiedebach, S. Bertrand, T. Wu, L. Fiorio, S. McCrory, R. Griffin, F. Nori, and J. Pratt. Walking on partial footholds including line contacts with the humanoid robot Atlas. In *IEEE-RAS International Conference on Humanoid Robots*, pages 1312–1319, nov 2016.

[9] D. N. Nenchev. Reaction Null Space of a multibody system with applications in robotics. *Mechanical Sciences*, 4:97–112, 2013.

[10] D. E. Orin and A. Goswami. Centroidal momentum matrix of a humanoid robot: Structure and properties. In *IEEE/RSJ International Conference on Intelligent Robots and Systems, IROS*, pages 653–659, Nice, France, 2008.

[11] D. E. Orin, A. Goswami, and S. H. Lee. Centroidal dynamics of a humanoid robot. *Autonomous Robots*, 35(2-3):161–176, 2013.

[12] S. H. Hyon, J.G. Hale, and G. Cheng. Full-body compliant human-humanoid interaction: balancing in the presence of unknown external forces. *IEEE Transactions on Robotics*, 23(5):884–898, oct 2007.

[13] B. Henze, M. A. Roa, and C. Ott. Passivity-based whole-body balancing for torque-controlled humanoid robots in multi-contact scenarios. *The International Journal of Robotics Research*, 35(12):1522–1543, oct 2016.

[14] D. N. Nenchev. Differential Kinematics. In Ambarish Goswami and Prahlad Vadakkepat, editors, *Humanoid Robotics: A Reference*. Springer Netherlands, Dordrecht, 2018.

[15] A. Liegeois. Automatic supervisory control of the configuration and behavior of multibody mechanisms. *IEEE Transactions on Systems, Man, and Cybernetics*, 7(12):868–871, 1977.

[16] 日向遼太郎，金宮好和: “反動零空間法に基づいた角運動量ダンパによる人型ロボットのバランス維持” (to be published)，日本ロボット学会学術講演会, 2018.

[17] A. Preumont. *Vibration Control of Active Structures*, volume 179 of *Solid Mechanics and Its Applications*. Springer Netherlands, Dordrecht, 3rd edition, 2011.

[18] 中村拓真，金宮好和: “反動零空間法を用いた回転台上での人型ロボットの全身モデルを用いた外乱に対するバランス制御” (to be published)，日本ロボット学会学術講演会, 2018.